

Published in final edited form as:

Chem Commun (Camb). 2010 October 7; 46(37): 6915–6917. doi:10.1039/c0cc01832e.

Multicolored redox active upconverter cerium oxide nanoparticle for bio-imaging and therapeutics†

Suresh Babu^a, Jung-Hyun Cho^b, Janet M. Dowding^c, Eric Heckert^c, Chris Komanski^d, Soumen Das^e, Jimmie Colon^d, Cheryl H. Baker^d, Michael Bass^b, William T. Self^c, and Sudipta Seal^{*,a,e}

^aAdvanced Materials Processing and Analysis Centre, Department of Mechanical, Materials and Aerospace Engineering, University of Central Florida, Orlando, FL 32816, USA

^bCenter for Research and Education in Optics and Lasers (CREOL), The College of Optics and Photonics, University of Central Florida, Orlando, FL 32816, USA

^cDepartment of Molecular Biology and Microbiology, Burnett School of Biomedical Sciences, University of Central Florida, Orlando, FL 32816, USA

^dM.D. Anderson Cancer Center Orlando, Cancer Research Institute, Orlando, FL 32806, USA

^eNanoScience Technology Center (NSTC), University of Central Florida, Orlando, FL 32816, USA

Abstract

Cytocompatible, co-doped cerium oxide nanoparticles exhibited strong upconversion properties that were found to kill lung cancer cells by inducing apoptosis thereby demonstrating the potential to be used as clinical contrast agents for imaging and as therapeutic agents for treatment of cancer.

Understanding the complex interactions of nanomaterials at the cellular level is required for proper designing of the nanoparticles for therapeutics. Fluorescent labeling is commonly used to study these interactions. The fluorophores commonly suffer from auto-fluorescence interference from biological tissues, photobleaching, low signal-to-noise ratio, potential damage to DNA and cell death.^{1,2} Though semiconductor quantum dots exhibit tunable size-dependent emission, some of the bare quantum dots possess intrinsic limitations such as toxicity and chemical instability. Therefore, developing nanoparticles of low toxicity with imaging as well as therapeutic properties is a key challenge in nanomedicine. Upconversion phosphors (UCPs), capable of converting near-infrared (NIR) radiation into shorter wavelengths through a multi-photon process, offer an alternative with minimal photo damage and auto-fluorescence due to the noninvasive nature of light.³ Since upconversion occurs within the host crystal and is therefore less affected by the chemical and biological environments, it allows synthesis of materials without the loss of surface chemical reactivity.

Metal fluorides, oxysulfides and phosphates are the host lattices widely used to study the upconversion process^{3–9} while only a few reports are available on oxide matrices.^{10,11} Among the metal oxide, rare earth oxides, in particular cerium oxide nanoparticles or ceria (CNPs)^{12,13} and europium hydroxide nanorods,^{14,15} have been shown to be biocompatible.

†Electronic supplementary information (ESI) available: X-ray diffraction of UNCs and Experimental details. See DOI: 10.1039/c0cc01832e

Beside biocompatibility CNPs are also reported to exhibit unique regenerative antioxidant properties.^{16–18} In this study, we synthesized rare earth co-doped CNPs with a sensitizer (Yb^{3+}) and an emitter (primarily Er^{3+}) having near-infrared (NIR)-to-visible upconversion fluorescence. To demonstrate the tunability of emission wavelength, the dopant chemistry was changed to Ho^{3+} or Tm^{3+} . Briefly, ammonia solution was added to aqueous nitrate solutions of Ce^{3+} (0.1 M), Yb^{3+} (20%) and Er^{3+} (2%), to maintain the pH above 10. The resultant upconversion nano cerium oxide (referred as UNC, hereafter) precipitate was washed, annealed at 900 °C for 2 h and filtered through 100 nm membrane filter.¹⁹ A similar procedure was used to synthesize $\text{CeO}_2 : 20\% \text{Yb}, 2\% \text{Ho}$ and $\text{CeO}_2 : 20\% \text{Yb}, 0.5\% \text{Tm}$. To evaluate the size and morphology high resolution transmission electron microscopy (HRTEM) studies were carried out with FEI Tecnai F30. Powder X-ray diffraction (XRD) was performed with monochromatized $\text{CuK}\alpha$ radiation.

UNCs have a primary particle size of about 20 nm along (see supporting information, Fig. 1S[†]) with a few particles in the size range of 40 nm due to the interfusion to form larger agglomerated particles. The presence of Yb and Er in cerium matrix was confirmed using Energy Dispersive X-ray analysis in TEM (see supporting information, Fig. 2S[†]).

Fig. 1 shows the absorption spectrum for UNC indicating the absorption feature at 975 nm (Fig. 1a) and emission spectra of UNC along with $\text{CeO}_2 : 20\% \text{Yb}, 2\% \text{Ho}$ and $\text{CeO}_2 : 20\% \text{Yb}, 0.5\% \text{Tm}$ (Fig. 1b and $\text{CeO}_2 : 20\% \text{Yb}, 0.5\% \text{Tm}$ alone shown in supporting information, Fig. 3S). The transition $^4\text{F}_{9/2} \rightarrow ^4\text{I}_{5/2}$ leads to a red emission in UNC with a small amount of green light (around 540 nm $^4\text{S}_{3/2} \rightarrow ^4\text{I}_{5/2}$ transition) due to Er^{3+} . On co-doping with Ho^{3+} green emission appears as a result of $^5\text{F}_4, ^5\text{S}_2 \rightarrow ^5\text{I}_8$ transition along with weak red light. Tm^{3+} co-doping results in weak blue emission ($^1\text{G}_4 \rightarrow ^3\text{H}_6$) due to lower probability for multi photon transitions.²⁰ UNC powders when excited by 975 nm light from the diode laser could be easily seen to emit red light (Fig. 1b inset). In earlier studies using fluoride hosts, the decay dynamics indicate a fluorescent lifetime of about 3 ms compared to 10.6 μs for UNC (Fig. 1c).²¹ The very short emission time observed in the present work indicates the presence of significant fluorescence quenching. Since oxide matrices have higher phonon energy than the fluorides this strong quenching is not surprising. In spite of quenching, the upconversion emission intensity is sufficient to utilize the water dispersible UNCs as potential biomarkers (Fig. 1d–g). Thus, the emission color can be tuned from red, green or blue by varying the co-dopant from Er^{3+} , Ho^{3+} and Tm^{3+} , respectively.

As mentioned earlier, CNPs can scavenge free radicals and mimic enzymatic antioxidants such as superoxide dismutase and catalase.^{17,18} We followed catalase mimetic activity of UNCs by monitoring peroxide levels using UV-visible spectrophotometry. In presence of 100 μM UNC, concentration of hydrogen peroxide reduced with time (see supporting information, Fig. 4S[†]). From this observation, it is evident that UNCs have redox activity similar to CNPs.

To examine the imaging capabilities of UNCs in a biological model for the first time, we exposed the cells (human umbilical vein endothelial cell; HUVEC and human lung fibroblasts cell line; WI-38) in cultured monolayers to varying doses of UNCs, and observed a concentration-dependent increase in visible light emission. Fig. 2 shows UNC treated cells upon excitation with a 975 nm light with a 4 ns pulse rate, 10 Hz pulse repeat rate and a pump power of 170 mW (detailed protocol in supplementary information[†]). Although UNCs have a visible emission, the important step towards the biomedical application is to assess the biocompatibility. For these studies we chose primary (HUVEC) as well secondary cell

[†]Electronic supplementary information (ESI) available: X-ray diffraction of UNCs and Experimental details. See DOI: 10.1039/c0cc01832e

line (WI-38). We assessed toxicity by the metabolic reduction of a tetrazolium dye (MTT) and by the release of lactate dehydrogenase (LDH) (see supplementary information for details[†]).

No significant toxicity was observed in WI-38 cells with UNC_s (up to 1000 μ M). Some toxicity was observed in HUVECs in a dose dependent manner when viability was determined by MTT assay, however no significant release of LDH occurred, suggesting the material caused a decrease in cellular metabolic rate without lysis of the cell membrane (Fig. 3).

In order to investigate the therapeutic application of UNC on cancer cells *in vitro*, lung cancer cells (CRL-5803) were cultured for 24 h and then the media was aspirated and replaced with fresh media containing various nanoparticle concentrations (0, 0.01 nM, 0.1 nM, 1 nM, 10 nM, 100 nM). Post 24 h treatment cell proliferation determined by the Cell Titer-Glo[®] Luminescent Cell Viability and Proliferation Assay (Promega; Madison, WI) and activation of apoptosis was determined by measuring the activation of caspase-3/7 *via* the Caspase-Glo[®] 3/7 Assay (Promega; Madison, WI).

In the case of CRL-5803, proliferation of cancerous lung cells decreased by 33.7% ($p < 0.0001$) when exposed to 100 nM of UNC (Fig. 4a). To determine if this decrease in cell proliferation and viability was due to an increase in the activation of apoptosis, caspase-3/7 activity was measured. Caspase-3/7 activity increased by 56.6% ($p = 0.012$) when exposed to 100 nM UNC (Fig. 4b). Therefore, under *in vitro* cell culture conditions, the cellular interactions of UNC_s differ between normal *versus* tumor cells and can be attributed to the differences in cell metabolism as well as cell structure.²² The mechanism of decrease in cell proliferation and induction of apoptosis in cancerous cells by UNC_s is currently under investigation however, redox active CNPs¹⁶ may induce apoptosis by producing reactive oxygen species and oxidative stress. Similar studies on TiO₂ nanoparticles have shown that they demonstrate cancer killing activity through ROS generation or surface interaction with cells.^{23,24}

In this study, we have demonstrated that co-doped cerium oxide nanoparticles exhibit a unique promising platform for *in vivo* optical-based diagnostic imaging and therapeutic agents. Nanoparticles are shown to be biocompatible using MTT and LDH assays with both primary and secondary cell lines. UNC_s interact in a cell specific manner preventing cancer cell proliferation by inducing apoptosis, which can have a far reaching impact in future cancer research. Use of non toxic upconverter oxide nanoparticles for imaging and therapeutic application is a novel platform technology. Tailoring the size, shape and surface can help in optimizing the clinical dosage and material property and will be discussed in future communications.

Supplementary Material

Refer to Web version on PubMed Central for supplementary material.

Acknowledgments

This work was supported by NSF NIRT (0708172 CBET) and NIH R01 (1R01AG031529-01).

Notes and references

1. Green M, Howman E. Chem. Commun 2005:121–123.
2. Riegler J, Nann T. Anal. Bioanal. Chem 2004:379.
3. Auzel F. Chem. Rev 2004;104:139–173. [PubMed: 14719973]

4. Chen F, Liu Y, Zhang Y, Somesfalean G, Zhang Z, Sun Q, Wang F. *Appl. Phys. Lett* 2007;91:133103.
5. Ehlert O, Thomann R, Darbandi M, Nann T. *ACS Nano* 2008;2:120–124. [PubMed: 19206555]
6. Zijlmans H, Bonnet J, Burton J, Kardos K, Vail T, Niedbala RS, Tanke HJ. *Anal. Biochem* 1999;267:30–36. [PubMed: 9918652]
7. Chatterjee DK, Rufaihah AJ, Zhang Y. *Biomaterials* 2008;29:937–943. [PubMed: 18061257]
8. Jalil RA, Zhang Y. *Biomaterials* 2008;29:4122–4128. [PubMed: 18675453]
9. Shan J, Chen J, Meng J, Collins J, Soboyejo W, Friedberg JS, Ju J. *J. Appl. Phys* 2008;104:094308.
10. Kamimura M, Miyamoto D, Saito Y, Soga K, Nagasaki Y. *Langmuir* 2008;24:8864–8870. [PubMed: 18652424]
11. Liu YX, Xu CF, Yang QB. *J. Appl. Phys* 2009;105:084701.
12. Thill A, Zeyons O, Spalla O, Chauvat F, Rose J, Auffan M, Flank AM. *Environ. Sci. Technol* 2006;40:6151–6156. [PubMed: 17051814]
13. Xia T, Kovoichich M, Liong M, Madler L, Gilbert B, Shi H, Yeh J, Zink J, Nel A. *ACS Nano* 2008;2:2121–2134. [PubMed: 19206459]
14. Patra CR, Abdel Moneim SS, Wang E, Dutta S, Patra S, Eshed M, Mukherjee P, Gedanken A, Shah VH, Mukhopadhyay D. *Toxicol. Appl. Pharmacol* 2009;240:88–98. [PubMed: 19616569]
15. Patra CR, Bhattacharya R, Patra S, Vlahakis NE, Gabashvili A, Kolytyn Y, Gedanken A, Mukherjee P, Mukhopadhyay D. *Adv. Mater* 2008;20:753–756.
16. Heckert EG, Karakoti AS, Seal S, Self WT. *Biomaterials* 2008;29:2705–2709. [PubMed: 18395249]
17. Korsvik C, Patil S, Seal S, Self WT. *Chem. Commun* 2007:1056–1058.
18. Pirmohamed T, Dowding JM, Singh S, Wasserman B, Heckert E, Karakoti AS, King JES, Seal S, Self WT. *Chem. Commun* 2010;46:2736–2738.
19. Babu S, Velez A, Wozniak K, Szydłowska J, Seal S. *Chem. Phys. Lett* 2007;442:405–408.
20. Rapaport A, Milliez J, Szipőcs F, Bass M, Cassanho A, Jenssen H. *Appl. Opt* 2004;43:6477–6480. [PubMed: 15617285]
21. Rapaport A, Milliez J, Bass M, Cassanho A, Jenssen H. *J. Disp. Technol* 2006;2:68–78.
22. Vincent A, Babu S, Heckert E, Dowding J, Hirst SM, Inerbaev TM, Self WT, Reilly CM, Masunov AE, Rahman TS, Seal S. *ACS Nano* 2009;3:1203–1211. [PubMed: 19368374]
23. Hanley C, Layne J, Punnoose A, Reddy K, Coombs I, Coombs A, Feris K, Wingett D. *Nanotechnology* 2008;19:295103–295110. [PubMed: 18836572]
24. Thevenot P, Cho J, Wavhal D, Timmons R, Tang L. *Nanomed.: Nanotechnol., Biol. Med* 2008;4:226–236.

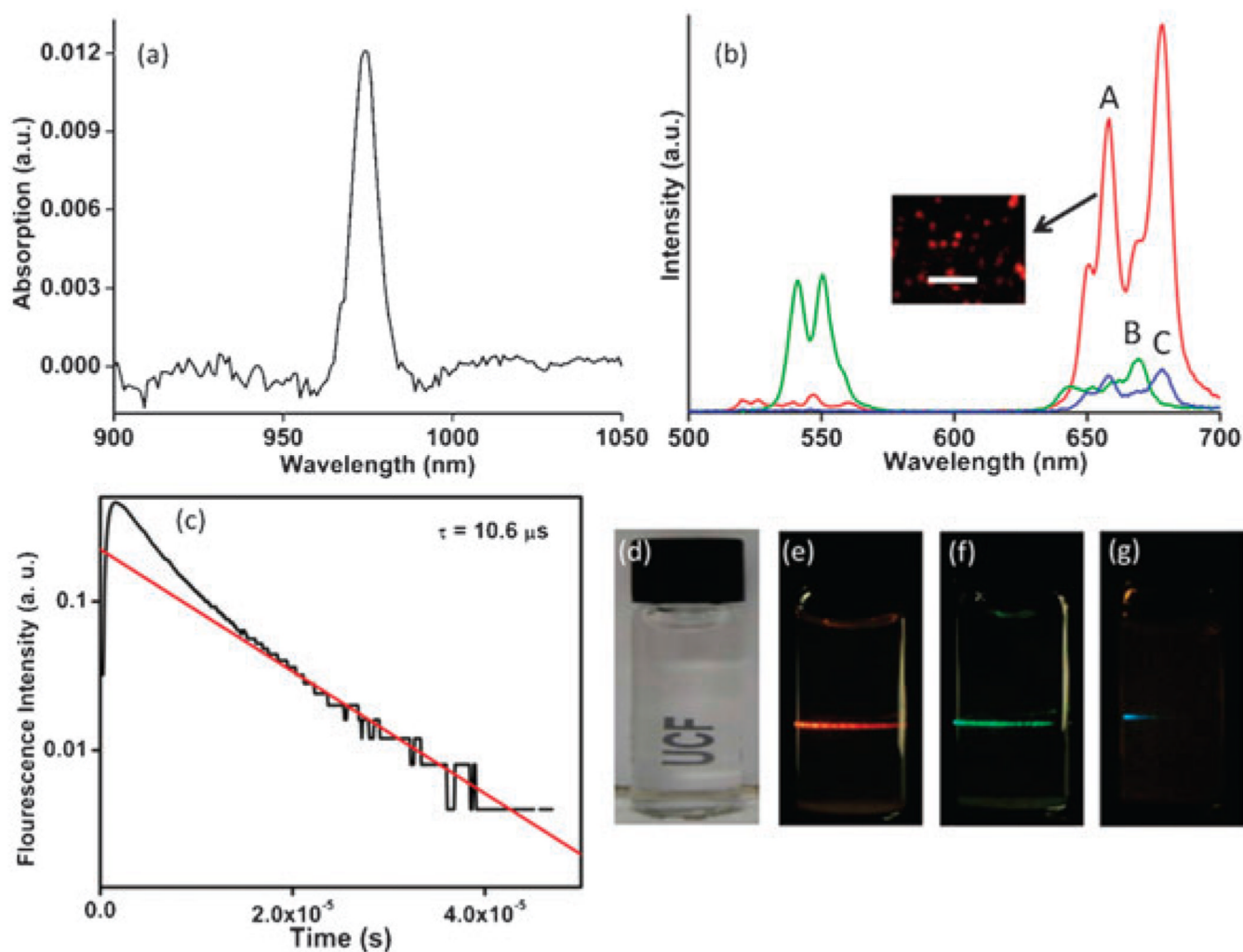


Fig. 1.

(a) The optical absorption spectrum of UNC. (b) The measured emission spectra of samples of (A) UNC, (B) CeO₂ : 20 Yb%,2%Ho and (C) CeO₂ : 20% Yb,0.5%Tm. The inset demonstrates the red emission from UNC observed under an optical microscope upon NIR excitation. Scale bar in the inset corresponds to 10 mm. (c) The measured emission decay dynamics of the red light emitted from UNC. The solid line is an exponential decay fit with decay time of 10.6 μsec. (d) Nanoparticles readily dispersed in water under visible light. (e–g) On NIR excitation (975 nm), emission wavelengths can be tuned from red, green or blue by varying the co-dopant chemistry from Er³⁺, Ho³⁺ or Tm³⁺, respectively.

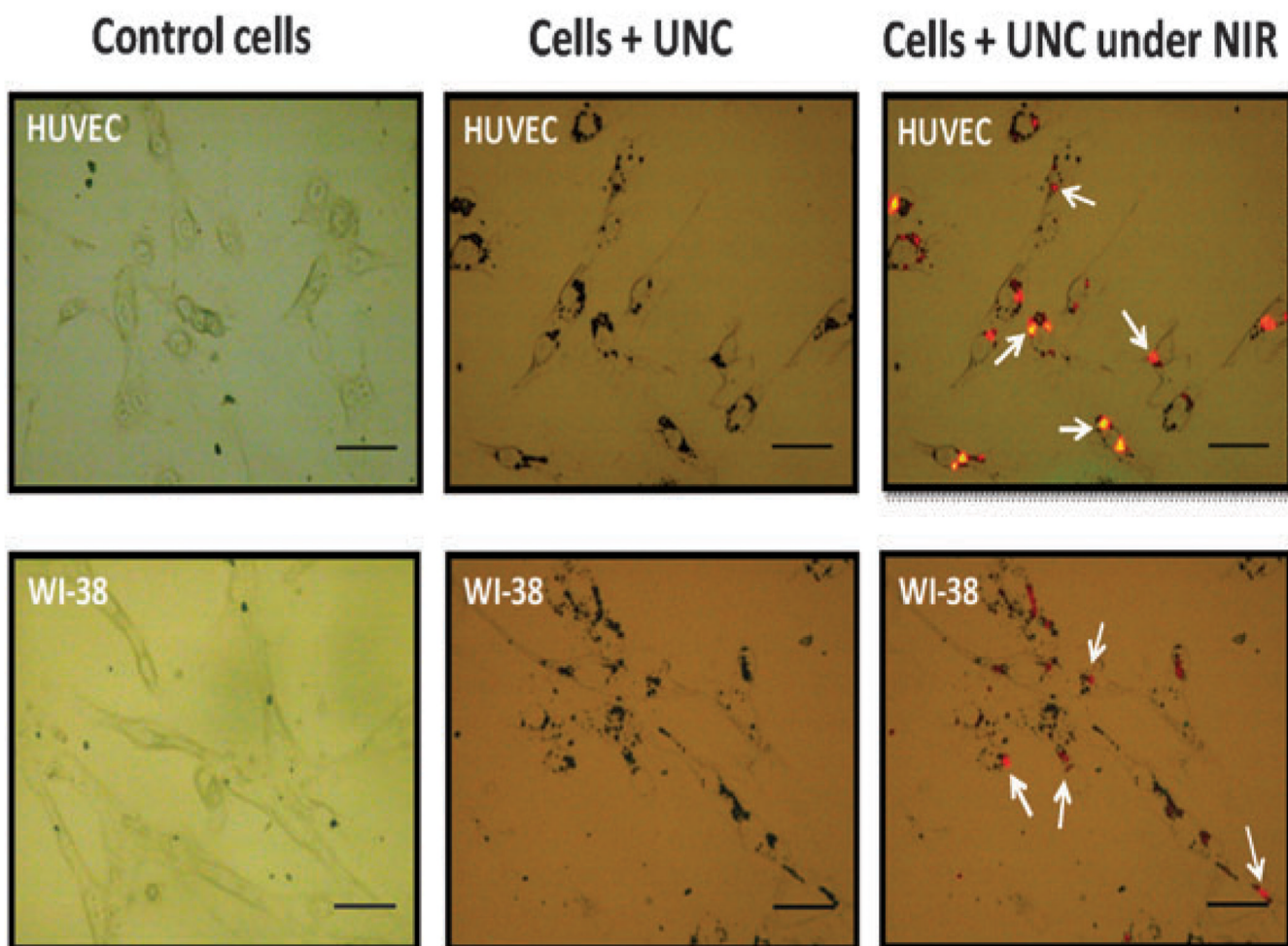


Fig. 2. Optical images of HUVEC and WI-38 control cells (without nanoparticles), along with cells incubated with UNC under ambient light and NIR excitation (scale bar corresponds to 50 μm). Arrowheads indicate the red emission from UNC when cells were excited at a wavelength of 975 nm.

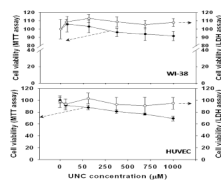


Fig. 3. UNCs are not toxic in cell culture models of WI-38 and HUVEC. Cells were cultured in their standard conditions. MTT dye reduction (●) and LDH release (○) was assessed after 24 h treatment with varying concentrations of UNC. Data represent the mean of at least six cultures and standard deviation is plotted as error.

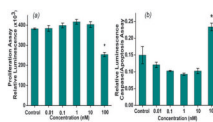


Fig. 4. (a) Cell viability of cancerous lung cells (CRL-5803) and (b) caspase 3/7 activation in cancer cells with respect to UNC concentration, at 100 nM the viability of cancer cells decreased and the data shown are mean \pm SD. Significant differences indicated by * with a p value of <0.0001 and 0.012 for a and b, respectively.